

Chance-constrained Solar PV Hosting Capacity Assessment for Distribution Grids Using Gaussian Process and Logit Learning

Sel Ly^a, Anshuman Singh^a, Petr Vorobev^a, Yeng Chai Soh^a and Hung Dinh Nguyen^{a,1}

^a*School of Electrical and Electronics Engineering, Nanyang Technological University, Singapore, 639798*

ARTICLE INFO

Keywords:

Hosting Capacity, Solar PV, Over-voltage, Gaussian Process, Chance constrained optimization, Logit learning.

ABSTRACT

Growing penetration of distributed generation such as solar PV can increase the risk of over-voltage in distribution grids, affecting network security. Therefore, assessment of the so-called, PV hosting capacity (HC) - the maximum amount of PV that a given grid can accommodate becomes an important practical problem. In this paper, we propose a novel chance-constrained HC estimation framework using Gaussian Process and Logit learning that can account for uncertainty and risk management. Also, we consider the assessment of HC under different voltage control strategies. Our results have demonstrated that the proposed models can achieve high accuracy levels of up to 93% in predicting nodal over-voltage events on IEEE 33-bus and 123-bus test-cases. Thus, these models can be effectively employed to estimate the chance-constrained HC with various risk levels. Moreover, our proposed methods have simple forms and low computational costs of only a few seconds.

Nomenclature

\mathcal{L}, \mathcal{G}	Sets of all loads and generators in the power network
$\beta \in (0, 1)$	Risk level for the over-voltage event
\mathbf{K}	Kernel matrix of the GP model
λ, τ	Hyperparameters of the GP kernel function
\bar{C}_k	Upper limit of the solar PV rated capacity installed at bus k
\mathcal{B}	The set of lines (branches) in the power network
C_k	The solar PV rated capacity installed at bus k
$\mu_f(x^*), \sigma_f^2(x^*)$	Predicted mean and variance values of V_{max} by the GPR, given the unseen PV level $X = x^*$
Ω	The set of correlated scenarios between solar irradiance and load demand
ω	Scenario from the uncertain set Ω
\bar{P}_d	Peak demand of the network (MW)
Φ	CDF of standard Gaussian distribution $\mathcal{N}(0, 1)$
θ_{kl}	Phase difference between buses k and l
$\underline{s}_{kl}, \bar{s}_{kl}$	Lower and upper limits of the apparent power flow
\underline{V}, \bar{V}	Lower and upper limits on voltage magnitudes
\tilde{V}	Binary variable indicating the over-voltage event

C_ρ	Gaussian copula with its parameter ρ
$f(x)$	The predictive GP model indexed by the PV level input $X = x$
N^b	The number of buses in the power network.
P_k, Q_k	Active/reactive power injections at bus k
$P_{d,k}/P_{g,k}$	Power demand / Solar PV generation at bus k
$P_{L,k}$	The net power injection (net load) at bus k
P_{nd}/P_{ng}	Normalized demand / Solar PV generation
PV^{loc}	The set of solar PV locations (PV buses)
$R(x)$	Predicted probability of the over-voltage event (risk index), given the PV level $X = x$
$S_{g,k}$	Apparent power generated by PV unit at bus k
s_{kl}	The apparent power flow between bus k and l
V_k, θ_k	Voltage magnitude and phase at bus k
V_{max}	Maximum of nodal voltage magnitudes
X	Ratio of the total PV installation capacity to the system peak load (PV level)
Y_{kl}	Element (k, l) of admittance matrix Y

Abbreviations

Below in Table 1, we provide a list of abbreviations/terminologies used in the paper.

Authors are with School of Electrical and Electronics Engineering, Nanyang Technological University, Singapore: {sel.ly, anshuman004, petr.vorobev, hunghtd}@ntu.edu.sg

ORCID(s):

¹Corresponding Author

Table 1
Abbreviations/terminologies.

Name	Meaning
CC	Chance-constrained.
CCO	Chance-constrained optimization.
HC	Hosting capacity.
GP	Gaussian process.
GPR	Gaussian process regression.
LoR	Logistic regression.
CDF	Cumulative distribution function.
MCS	Monte Carlo simulation.
PV	Photovoltaic.
RES	Renewable energy source.
DER	Distributed energy resource.
GP-WoCC-HC	Mean and bounds of HC estimations resulting from the GP learning without considering CCO.
GP-CC-HC	HC estimations resulting from the GP learning and CCO.
Logit-CC-HC	HC estimations resulting from the logit learning and CCO.
PCE-CC-POPF	Polynomial chaos expansion-based chance-constrained probabilistic optimal power flow.
Q control	Droop-based reactive power control.
PF control	Droop-based power factor control.
ESS control	Droop-based energy storage system control.

1. Introduction

Integrating renewable energy sources (RESs) such as solar PV at the distribution network is a key element in the transition towards a more sustainable and resilient energy future [42]. However, a technical limit exists on the maximum amount of RESs that can be installed in a network. This limitation is primarily attributed to over-voltages caused by reverse power flows [47, 15]. As RESs at the distribution level are non-dispatchable, these reverse power flows cannot be effectively managed or controlled. Thus, to assess the impact of RESs on the network, it is essential to perform an estimation of the so-called, network's hosting capacity (HC), i.e. the maximum amount of distributed generation that can be connected to the network without violating its operational limits and without the need for network expansion [32].

Overestimation of HC can lead to grid instability, increased likelihood of power outages, and potential damage to equipment [23, 2]. On the other hand, underestimation of HC can lead to the under-utilization of the grid capabilities to host RES, which can impact the economic viability of renewable energy projects and delay the transition towards a more sustainable energy future. Thus, it is essential to perform an accurate estimation of the network's HC for maintaining grid stability and ensuring safe, reliable operation.

Stochastic estimation of HC can be performed through Monte Carlo (MCS) simulation-based methods which include the generation of a large number of location-size scenarios for a given PV penetration level, followed by load flow analysis of each scenario. Frameworks to estimate HC by the MCS method have been proposed in works [13, 3, 12].

However, MCS-based methods only generate a small fraction of location-size scenarios out of all possible combinations. Hence, these methods need to be re-run multiple times to obtain confidence bounds on the HC value, resulting in thousands of MC simulations. Additionally, the above works do not consider the uncertainties of load and PV output, and only worst-case scenarios are considered, i.e. maximum RES output and minimum load obtained from historical data. This results in a conservative estimation of the network's HC.

Various methods have been proposed to address the uncertainty in load and generation for MCS-based HC estimation frameworks. Approaches include probabilistic modelling of demand and generation using various distributions [4], interval and affine arithmetic [31], possibilistic methods with membership functions [50], and Herman-Beta extended transform-based probabilistic power flow [9]. Authors in [46] have proposed a Monte Carlo-based approach for evaluating the PV hosting capacity of a three-phase unbalanced network. In this work, the maximum voltage for each location-size scenario is obtained and an interval distribution for this relationship is constructed. The HC is evaluated such that the probability of overvoltage is within a given interval. However, these studies do not account for the correlation between load and Distributed Energy Resource (DER) generation, which can impact reliability assessment, as highlighted in [39]. While [43] introduces an HC method considering correlated uncertainties, it assumes predefined locations for renewable energy sources.

The optimization-based hosting capacity estimation have also been proposed in prior works. In this formulation, the objective is to maximize the installed capacity of DERs, subject to power flow equations and network operational constraints, such as voltage limits. This approach has been used in works [19, 53, 10]. However, one limitation of this method is that the optimization algorithm selects the location and size of DER in a way that maximizes the objective while satisfying all constraints. Hence, the resulting solution represents one possible optimal configuration and skips all other possible configurations that can potentially violate system constraints. This approach assumes that the system operator has control over DER placement and sizing, which might not reflect real-world scenarios where it is driven by the end-user decisions. As a result, the optimal solution obtained from the optimization problem might not reflect realistic DER placement scenarios, potentially leading to over-estimation of the true hosting capacity.

The HC can also be evaluated by methods other than load flow and optimization-based frameworks. An alternative approach to estimate HC has been proposed in [44]

using smart meter data and voltage sensitivities. However, the HC evaluated here is only for one bus at a time. Further, authors in [33, 28] have utilized voltage sensitivities to estimate the over-voltage violations and the HC for the network. However, the sensitivity methods include linearization of the power system model and may not accurately capture the non-linear behavior of the network under all conditions. Authors in [26] have developed the HC problem as an optimization model that finds the locations that tend to be the worst for the DG integration and then maximizes the DG size for these locations. However, it leads to a conservative estimate of the HC. Authors in [55] have proposed a distributionally robust chance constraint (DRCC) optimization method to construct a feasible region for PV integration, given the set of candidate locations. In this work, the operational limits on voltage are converted to a DRCC model satisfying a given probability. Further, the PV output uncertainty is modeled by a data-driven Wasserstein-based ambiguity set. Authors in [54] have further utilized the DRCC-based feasible region construction for a net-zero distribution system having battery energy storage systems.

Apart from the estimation of the HC, there is a problem of increasing HC through additional measures, such as voltage control. This can include, for example, reactive power support from PV inverters. Numerous papers confirm a smart control of PV inverters that can help regulate nodal voltages, thus increasing the HC of a grid [38, 22]. Hence, in this work, we also use our proposed framework to analyze the impact of different voltage control approaches on the network's HC.

Considering the large amount of time taken by MCS-based frameworks, we aim to develop a novel HC estimation methodology using a chance-constrained optimization (CCO) approach based on the Gaussian Process regression (GPR) and logistic regression (LoR). There are multiple advantages of using CCO approach over robust optimization and scenario-based optimization. The robust optimization method ensures feasibility in all scenarios leading to a conservative solution and is computationally difficult [16]. On the other hand, CCO only requires satisfying system constraints with a certain confidence level, making it more practical [18]. Scenario-based optimization struggles with the accuracy-complexity trade-off, where too many scenarios slow down the process, while too few lead to poor results.

GPR is a well-known machine learning algorithm known for its ability to effectively approximate smooth non-linear functions while providing a favourable balance between accuracy and complexity [27, 41]. The GPR-based frameworks have been used before to learn power flow [37], optimal power flow [30, 36], and battery health prediction [14].

The motivations for using CCO approach along with GPR and LoR are as follows:

- i. **Risk management:** The chance-constrained framework will allow us for flexible risk management by controlling the probability of constraint violations. This adaptability is crucial for the distribution system

operators, enabling them to quickly tailor the risk tolerance according to their specific needs.

- ii. **Uncertainty quantification:** Instead of giving a single deterministic output, GPR provides a predictive mean and variance for each test point. The variance quantifies the uncertainty in the prediction. Similarly, LoR can also classify whether a given PV penetration level will lead to over-voltage or not with a certain probability.
- iii. **Cost-effectiveness:** The proposed models are computationally efficient and scalable with advanced techniques, such as sparse GPs and variational inference. By using these techniques, we can process and analyze large data, corresponding to a large number of possible scenarios, allowing for enhancing the accuracy and reliability of chance-constrained HC assessments.
- iv. **Flexibility and interpretability:** GPR and LoR are flexible and interpretable modeling techniques. Especially, the GPR, being non-parametric, can accommodate any form of input uncertainty without requiring the knowledge of the uncertainty distribution.
- v. **Sensitivity Analysis:** Although HC estimation is a planning problem, the computational time is crucial for sensitivity analysis. For example, to assess HC reduction if bus 4 is unavailable for solar PV, Monte Carlo methods require a full re-run. In contrast, the proposed method uses probabilistic machine learning techniques like GPR and LoR, which require fewer samples and provide quicker results.

By developing and validating a novel methodology for estimating the hosting capacity, this research will contribute to the development of a more sustainable and resilient energy future. The findings of this research will be valuable to stakeholders in the power sector, including policymakers, regulators, utilities, and renewable energy developers.

The main contributions of the manuscript are as follows:

1. Develop a novel chance-constrained HC estimation technique that accounts for both location and operational uncertainties. We also incorporate the correlation between the load demand and the PV generation using the copula theory.
2. Develop a Gaussian process learning framework to quantify the impacts of the PV penetration level on the voltage distribution. We also develop a logistic regression-based HC estimation model and compare its effectiveness with the GPR model. With the use of GPR and LoR, the chance-constrained HC estimation method can be reformulated in a very simple form which offers a fast and scalable solution.
3. Analyze the effect of various voltage control techniques on the HC assessment such as droop-based PV

inverter control and energy storage system control, using the proposed framework.

The rest of the paper is structured as follows. Section 2 details the HC estimation problem. In section 3, we propose two main HC estimation methods with/without considering chance constraints of over-voltage issues, which are based on the GPR and LoR. Section 4 presents the results and discussions. The data generation process along with PV inverter/ ESS control schemes are discussed in the Appendix.

2. Problem formulation

We will start this section by introducing the probabilistic load flow (PLF) model to obtain samples of PV output and corresponding maximum voltage. We then formulate the chance-constrained optimization for the HC estimation. For improved readability, we have moved the details of the data generation process and the control methods to the Appendix which is present at the end of this paper.

2.1. Load flow model

The power flow equations can be defined as [34]

$$P_k + jQ_k = V_k \sum_{l=1}^{N^b} Y_{kl} V_l \exp(-j\theta_{kl}), \quad k \in \mathcal{L}, \mathcal{G}. \quad (1)$$

The notations are defined below:

- P_k/Q_k : active/reactive power injections at bus k .
- V_k, θ_k : voltage magnitude and phase at bus k .
- $\theta_{kl} = \theta_k - \theta_l$: phase difference between buses k and l .
- Y_{kl} : element (k, l) of admittance matrix Y .
- \mathcal{L} and \mathcal{G} are sets of all loads and generators in network.

Here, N^b denotes the number of buses. The net power injection (net load) at bus k can be given by: $P_{L,k} := P_{d,k} - P_{g,k}$. In case of additional components e.g. an ESS, the net injection can include power injection from that device too. We aim to capture the correlation between PV generation and demand. To achieve this, we use a copula function to model their joint cumulative distribution function (CDF). Later, the representative samples of load and demand are generated by drawing random samples from the estimated copula followed by inverse CDF calculation. For more details on the simulation setup and data generation, please refer to the Appendix.

2.2. Problem formulation of the HC estimation

In this section, we first briefly introduce the HC estimation problem. Let X denote the level of renewable penetration defined as the ratio of installed PV capacity to the system peak load demand power \bar{P}_d (MW):

$$X := \sum_{k \in PV^{loc}} \mathcal{C}_k / \bar{P}_d, \quad (2)$$

where \mathcal{C}_k is the PV rated capacity (MW) installed at bus k , and PV^{loc} denotes the set of potential buses where PV units may be installed. The hosting capacity (HC) can be estimated by considering the following maximization problem [8]:

$$HC := \max_{X \in (0,1)} X \quad (3a)$$

$$\text{s.t. Power Flow (1),} \quad (3b)$$

$$P_{g,k}^2 + Q_{g,k}^2 \leq S_{g,k}^2, \quad k \in \mathcal{G}, \quad (3c)$$

$$S_{g,k} \leq \mathcal{C}_k, \quad k \in PV^{loc}, \quad (3d)$$

$$\underline{\mathcal{C}}_k \leq \mathcal{C}_k \leq \overline{\mathcal{C}}_k, \quad k \in PV^{loc}, \quad (3e)$$

$$\underline{V} \leq V_k \leq \overline{V}, \quad k \in \mathcal{L}, \quad (3f)$$

$$\underline{s}_{kl} \leq s_{kl} \leq \overline{s}_{kl}, \quad k, l \in \mathcal{B}. \quad (3g)$$

Here, s_{kl} is the apparent power flow between bus k and l with \mathcal{B} being the set of lines (branches) in the network. Constraint (3c) denotes the capability curve of the PV inverter with $S_{g,k}$ representing the apparent power through the PV unit at bus k . \mathcal{C}_k is the rated capacity of the PV unit to be installed at bus k with $\overline{\mathcal{C}}_k$ being the given upper limit. In the presence of other devices such OLTC, energy storage, etc. the respective device model can be added [1, 49]¹. Underline and overline represent the lower and upper operational limit on the variable, respectively. Later, in the proposed framework, we do not consider explicitly the under-voltage since the maximum PV penetration is limited by over-voltages due to reverse power flow [35]. However, this can be added to the problem formulation at almost no additional cost. The counterpart on the line flow limits can be treated similarly.

2.3. Formulation of CC-HC estimation

In this section, we reformulate the deterministic HC problem (i.e. (3)) into the chance-constrained optimization model. Firstly, the stochastic nature of normalized power consumption P_{dn} at each bus is modelled using normal distribution $P_{dn} \sim N(\mu_d, \sigma_d^2)$. We further model the uncertain solar PV output using *Beta* distribution $P_{gn} \sim Beta(\alpha_{pv}, \beta_{pv})$. The probability density function of PV generation is found to be well approximated by a beta distribution [17]. Note that these normalized variables (P_{dn}, P_{gn}) can be multiplied with base values to obtain load P_d and PV output P_g .

We reformulate the hard limits on voltage (i.e. (3f)) to chance-constrained formulations as [52]:

$$\mathbb{P}(V_{max} \leq \overline{V} | X = x) \geq 1 - \beta, \quad (4)$$

where $V_{max} := \max_{1 \leq k \leq N^b} \{V_k\}$. It should be noted that \overline{V} is the operational limit on bus voltages (i.e. 1.05 p.u.). \mathbb{P} is the probability and β is the risk level ($\beta \in (0, 1)$).

¹It should be noted that in the presence of other control devices such as capacitor banks, OLTC, etc., more constraints can be added. However, the objective of this work is to develop a generalized HC estimation framework instead of finding the optimal set-point for control devices. Hence, we have ignored them. However, they can be added to the proposed framework without any difficulty.

The chance-constrained HC estimation (CC-HC) can be formulated as follows:

$$\text{CC-HC} := \max_{x \in (0,1)} x \quad (5a)$$

$$\text{s.t. } P_k^\omega + jQ_k^\omega = V_k^\omega \sum_{l=1}^{N^b} Y_{kl} V_l^\omega \exp(-j\theta_{kl}^\omega), \quad k \in \mathcal{L}, \mathcal{G}, \quad (5b)$$

$$(P_{g,k}^\omega)^2 + (Q_{g,k}^\omega)^2 \leq (S_{g,k}^\omega)^2, \quad k \in \mathcal{G}, \quad (5c)$$

$$S_{g,k}^\omega \leq \mathcal{C}_k^\omega, \quad k \in PV^{loc}, \quad (5d)$$

$$\mathcal{C}_k^\omega \leq \bar{\mathcal{C}}_k, \quad k \in PV^{loc}, \quad (5e)$$

$$\mathbb{P}(V_{max} \leq \bar{V} | X = x) \geq 1 - \beta, \quad (5f)$$

where $\omega \in \Omega$ represents a scenario from the uncertain set.

Solving (5) is difficult due to multiple reasons including computation intractability, uncertain location and size of future PV units, uncertain demand and PV output, etc. Furthermore, the non-linear nature of power flow equations adds an additional layer of complexity to the problem. Different models of power flow such as the DistFlow models can be used that reduce the complexity. However, the main challenge in solving this optimization problem is that the future locations of the solar PV units are uncertain, making the location a random variable.

Instead of directly solving the stochastic optimization problem (5), we adopt a different approach with three stages. **In stage 1:** We generate random scenarios for solar PV installation along with the correlated scenarios for solar PV output and load. Then we run the probabilistic load flow (1) to obtain a training dataset consisting of the PV penetration (X) as input and the maximum of all bus voltages (V_{max}) as output (see Appendix for more details on how we generate the data). **In stage 2:** using this dataset, we construct a predictive function $V_{max} = f(X)$ (through Gaussian Process modeling). Finally, **in stage 3:** we define a risk index based on voltage distribution as:

$$R(x) := \mathbb{P}(V_{max} > 1.05 | X = x), \quad (6)$$

Once the model of (6) is known, the HC problem i.e. (5) is transferred to:

$$\text{CC-HC} := \max_{x \in (0,1)} x \quad \text{s.t.} \quad R(x) \leq \beta, \quad (7)$$

for some risk level $\beta \in (0, 1)$. In this study, we consider several risk levels, including $\beta = 1\%$, 5% , and 10% , and we set the voltage limit $\bar{V} = 1.05$ (p.u.). The overall process flow is shown in Fig. 1.

However, the computation of the conditional probability (6) is a nontrivial task as we do not know the exact form and it is impossible to consider the whole possible outcomes of the continuous random variables X and V_{max} . Thus, it motivates us to leverage probabilistic machine learning models with available data. Specifically, we propose to use GPR and LoR models in this work.

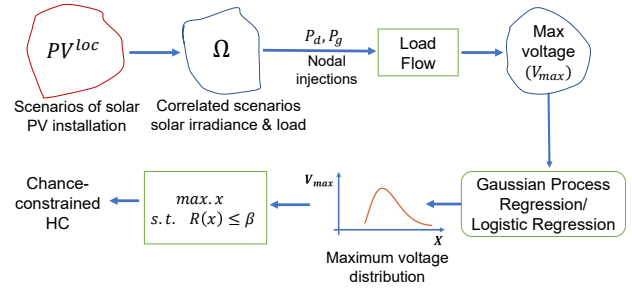


Figure 1: Process Flowchart for the proposed HC estimation framework.

3. Proposed methods

In this section, we first develop the GP-based chance-constrained HC estimation method. Recall that the Gaussian process is a collection of random variables, any finite number of which have a joint multivariate Gaussian distribution. While GP is a general framework for modelling distributions over functions, GPR is a specific application of GPs for regression tasks [48]. Unlike traditional regression methods, GPR does not assume a specific functional form, but uses a GP as a prior over functions and combines it with new input data to make predictions, along with uncertainty quantification [30]. Thus, GPR is a non-parametric probabilistic model and capable of handling complex non-linear input-output relationships. Later, we also develop the logistic regression-based CC-HC estimation method and compare the efficiency of both methods in section 4.

3.1. GPR-based HC estimation methods

Suppose we have a training sample of (X, V_{max}) denoted by $(x_1, \dots, x_n)^T$ and $(v_{max,1}, \dots, v_{max,n})^T$, where n is the sample size. Recall that X here refers to the PV penetration level (refer to (2)) and V_{max} refers to the maximum voltage among all buses. Without loss of generality, let us center the output V_{max} to have a zero mean by subtracting it from its sample mean $m := \frac{1}{n} \sum_{i=1}^n v_{max,i}$ as $y_i := v_{max,i} - m$. We are seeking a predictive function $f(x)$ such that:

$$y_i = f(x_i) + \varepsilon_i, \quad (8)$$

where ε denotes the noise term with zero mean and constant variance σ_ε^2 . Here, we model $f(x)$ as a GP defined as a collection of latent variables indexed by the input x and having joint multivariate Gaussian distribution [48]. In GPR, it combines prior and likelihood probabilities to derive posterior and predictive distributions, see e.g. [48] in detail. Suppose the new prediction is y^* using a new input x^* , conditional on the training observation $(x_i, y_i), i = 1, \dots, n$. This can be done by using the key predictive distribution of $f^* = f(x^*)$ determined by:

$$p(f^* | \mathbf{x}, \mathbf{y}, x^*) \simeq \mathcal{N}(\mu_f(x^*), \sigma_f^2(x^*)), \quad (9)$$

with the mean and variance functions defined by [48]:

$$\mu_f(x^*) := \mathbf{K}_*^T (\mathbf{K} + \sigma_\varepsilon^2 \mathbf{I})^{-1} \mathbf{y}, \quad (10)$$

$$\sigma_f^2(x^*) := \mathbf{K}_{**} - \mathbf{K}_*^T (\mathbf{K} + \sigma_\varepsilon^2 \mathbf{I})^{-1} \mathbf{K}_*. \quad (11)$$

where \mathbf{I} is the unit matrix of size $n \times n$, \mathbf{K} denotes the training kernel matrix of size $n \times n$, \mathbf{K}_* the training-testing kernel matrix of size $n \times 1$, and \mathbf{K}_{**} is the testing kernel matrix of size 1×1 , which can be explicitly calculated as follows, for example, if using "squared exponential kernel":

$$\begin{aligned} \mathbf{K}(x_i, x_j) &= \lambda^2 \exp\left(-\frac{(x_i - x_j)^2}{\tau^2}\right), \quad i, j = 1, \dots, n, \\ \mathbf{K}_*(x_i, x^*) &= \lambda^2 \exp\left(-\frac{(x_i - x^*)^2}{\tau^2}\right), \quad i = 1, \dots, n, \\ \mathbf{K}_{**}(x^*, x^*) &= \lambda^2 \exp\left(-\frac{(x^* - x^*)^2}{\tau^2}\right) = \lambda^2, \end{aligned}$$

where the variance of the noise σ_ε^2 , the hyper-parameters (λ^2, τ^2) of the kernel function are estimated from the training data $(x_i, y_i)_{i=1}^n$ by maximizing the log marginal likelihood, see (2.30) in [48].

To get back the original scale prediction for the new output v_{max}^* given on the new input x^* , we simply calculate the mean $\mu(x^*)$ and variance $\sigma^2(x^*)$ functions of $v_{max}^* = y^* + m$, with $y^* = f(x^*) + \varepsilon$:

$$\mu(x^*) = \mu_f(x^*) + m, \quad \sigma^2(x^*) = \sigma_f^2(x^*) + \sigma_\varepsilon^2. \quad (12)$$

In practice, $\mu(x^*)$ is used as a point prediction. Suppose we desire a prediction interval with a confident level of $(1 - \alpha) \times 100$ (%). This can be evaluated as

$$\mu(x^*) \pm z_{\alpha/2} \sigma(x^*), \quad (13)$$

where $z_{\alpha/2}$ is the upper quantile of standard normal distribution at level $\alpha/2$.

3.1.1. GPR-based HC estimation method for mean and confidence interval bounds

By utilizing the learned GPR, we now can reformulate the HC estimation considering the over-voltage issue in (3f) as follows:

$$\text{GP-WoCC-HC} := \max_{x^* \in (0,1)} \{x^*\} \quad \text{s.t.} \quad \mu(x^*) \leq 1.05, \quad (14)$$

where $\mu(x^*)$ is defined as in (12). In this work, we shall refer to the solution of (14) as the mean **GP-WoCC-HC**, i.e., the average HC estimation resulting from the GP learning without considering chance constraints.

Further, the GPR approach can also offer us both the lower and upper bounds for the HC estimation by utilizing the prediction interval (PI) (13):

$$\begin{aligned} \text{HC bounds} &:= \max_{x^* \in (0,1)} \{x^*\} \\ &\quad \text{s.t.} \quad \mu(x^*) \pm z_{\alpha/2} \sigma(x^*) \leq 1.05, \end{aligned} \quad (15)$$

for given a confident level: $(1 - \alpha) \times 100$ %.

3.1.2. GPR-based CC-HC estimation method

Now, to develop the HC estimation with chance constraints, we calculate the probability of constraint violation or the risk index in (6) as:

$$\mathbb{P}(V_{max} > 1.05 | X = x^*) = 1 - \Phi\left(\frac{1.05 - \mu(x^*)}{\sigma(x^*)}\right). \quad (16)$$

Then, we can reformulate the chance-constrained HC estimation in (7) based on this GP learning (**GP-CC-HC** for short) as:

$$\begin{aligned} \text{GP-CC-HC} &:= \max_{x^* \in (0,1)} \{x^*\} \\ &\quad \text{s.t.} \quad \mu(x^*) + \sigma(x^*) \Phi^{-1}(1 - \beta) \leq 1.05, \end{aligned} \quad (17)$$

for some risk level $\beta \in (0, 1)$, where $\mu(x^*)$ and $\sigma(x^*)$ are the predicted mean and standard deviation of the V_{max} through the learned GPR defined as in (12), and Φ^{-1} denotes the inverse CDF (quantile function) of the standard normal distribution.

3.1.3. A relationship between GP-WoCC-HC and GP-CC-HC estimation methods

Note that if we take $\beta = \alpha/2$, then we have

$$\Phi^{-1}(1 - \beta) = \Phi^{-1}(1 - \alpha/2) = z_{\alpha/2}, \quad (18)$$

and thus, the **GP-CC-HC** problem in (17) with a risk level of β is equivalent to the lower bound of the **GP-WoCC-HC** problem in (15) with the confidence level of

$$(1 - \alpha) \times 100(\%) = (1 - 2\beta) \times 100(\%).$$

Next, for a simple comparison purpose with the proposed GP learning, we provide another approach using the so-called logit learning.

3.2. LoR-based CC-HC estimation method

Another approach to compute the risk (6) is via logistic regression. To do so, we begin by defining the following violation variable:

$$\tilde{V} = \begin{cases} 1, & \text{if } V_{max} > 1.05, \\ 0, & \text{if otherwise.} \end{cases} \quad (19)$$

Then we can learn the conditional violation probability by using the logistic regression model of the form:

$$\mathbb{P}(\tilde{V} = 1 | X = x^*) = 1 / (1 + \exp(-\hat{b}_0 - \hat{b}_1 x^*)), \quad (20)$$

where \hat{b}_0 and \hat{b}_1 are the estimated parameters of the logistic regression using the training data (x_i, \tilde{v}_i) , $i = 1, \dots, n$. We now can determine the chance-constrained HC such that $\tilde{R}(x^*) := \mathbb{P}(\tilde{V} = 1 | X = x^*) \leq \beta$, i.e.,

$$\max_{x^* \in (0,1)} \{x^*\} \quad \text{s.t.} \quad 1 / (1 + \exp(-\hat{b}_0 - \hat{b}_1 x^*)) \leq \beta, \quad (21)$$

for some risk level $\beta \in (0, 1)$. Or equivalently, we have in terms of the logit representation:

$$\begin{aligned} \text{Logit-CC-HC} &:= \max_{x^* \in (0,1)} \{x^*\} \\ \text{s.t. } &\hat{b}_0 + \hat{b}_1 x^* \leq \text{logit}(\beta), \quad (22) \end{aligned}$$

where $\text{logit}(\beta) := \log\left(\frac{\beta}{1-\beta}\right)$, for some risk level $\beta \in (0, 1)$. We shall refer to this approach as the **Logit-CC-HC** method, i.e. logit-based chance-constrained HC estimation.

4. Results and discussions

In this section, we evaluate the proposed models. The load flow analysis was performed using the Matpower toolbox. The data generation process along with the PV inverter/ESS control schemes are given in the Appendix.

4.1. Test system

A modified IEEE 33-bus [5] and 123-bus [6] networks were used as test systems. The 33-bus network contained 2 capacitor banks of size 0.4 MVar at buses 18 and 33. The peak load in this network is 3.715 MW, 2.3 MVar with a base voltage of 12.66 kV. The 123-bus network was equipped with capacitor banks of size 0.4, 0.4, and 0.2 MVar at bus 51, 61, and 64, respectively. The peak load in this network is 3.51 MW, 1.93 MVar with a base voltage of 4.16 kV. In both the networks, the point of common coupling (PCC) voltage was set at 1.03 p.u. to ensure that the lowest bus voltage is above 0.95 p.u. under the peak load condition. Simulations were performed on a computer with an Intel Xeon processor 3.7 Ghz, 16 GB RAM, and using MATLAB 2019a.

We considered 3000 location-size scenarios of PV installation. Further, we considered 4 representative load-generation profiles for each location-size scenario resulting in a total of 12000 scenarios to be analyzed using load flow analysis. We selected the period between 12 to 1 p.m. for analysis as it usually observes high sunshine and low residential demand, thus capturing the high bus voltages caused by solar PV [11]. This also ensures that the resulting HC estimate will not cause over-voltage violations for any load pattern on weekdays or weekends.

The historical PV output data was collected from the Photovoltaic Geographical Information System (PVGIS) toolbox [20] for the year 2020. The data was fitted on *Beta* distribution and the obtained shape parameters (α_{pv} and β_{pv}) were approximately equal to 15 and 6. It should be noted that β_{pv} is restricted to PV output and should not be confused with risk parameter β . Further, the normalized load was considered to be following a normal distribution with mean (μ_d) and standard deviation (σ_d) equal to 0.5 and 0.025 p.u. respectively. The Pearson's correlation coefficient was considered as 0.15. The resulting 4 representative load-generation pairs obtained from Module 1 (see Appendix) are [(0.54-0.96), (0.52-0.95), (0.51-0.93), (0.47-0.92)] with all values in per unit. The load and PV output at each bus were scaled using these values. The load flow analysis was

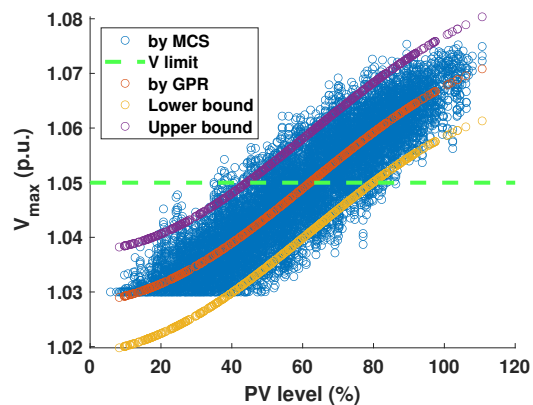


Figure 2: GPR used for predicting V_{max} on IEEE 33-bus system, given different PV penetration levels, in comparison to Monte Carlo simulation (MCS).

Table 2

Performance evaluations of GPR and LoR models on the testing data of 11500 samples.

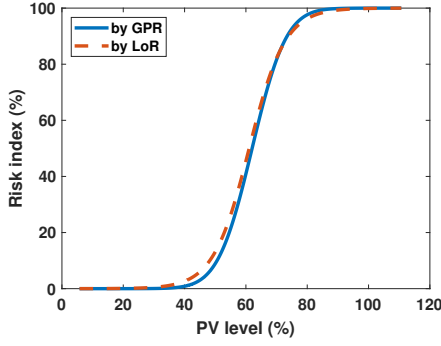
IEEE	Model	MAE	RMSE	R^2	Acc.
33-bus	GPR	0.0037	0.0047	85.76%	89.96%
	LoR	–	–	–	89.95%
123-bus	GPR	0.0021	0.0025	92.91%	93.01%
	LoR	–	–	–	93.01%

performed for each scenario with and without considering the control action.

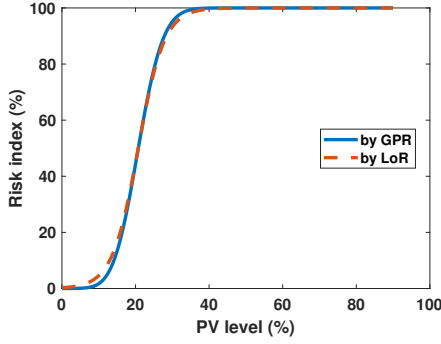
4.2. Evaluating the proposed models

Firstly, Fig. 2 plots the trained GPR with 500 random samples of the PV level input, in comparison to the Monte Carlo (MC) simulation of 12000 samples on the IEEE 33-bus network. The rest of the 11500 samples will be used as testing data. As can be seen, the GPR can be used for point predictions as well as for providing the lower and upper bounds (95% PI) of the maximum voltage output V_{max} . The error point predictions are small, with the mean absolute error (MAE) of only 0.0037 and 0.0021 (p.u.), performed on the IEEE 33-bus and 123-bus systems, respectively, as shown in Tab. 2. We also achieve high coefficients of determination R^2 , around 85.76% – 92.91% regarding the regression task. Not only can GPR be applied for forecasting the continuous random variable V_{max} , but it can also be utilized for classifying the event experiencing the over-voltage. This can be done by calculating the risk index $R(x^*)$ as in (16) for GPR and (20) for LoR. Specifically, given an integration of PV level $X = x^*$, we predict the likelihood of the over-voltage $R(x^*)$ and then classify it as an over-voltage violation if $R(x^*) > 0.5$. Tab. 2 shows that the classification accuracy (**Acc.**) by the GPR model is around 89.96% for IEEE 33-bus and 93.01% for IEEE 123-bus, performed on the testing data of 11500 samples. The logistic regression models perform similarly on the classification task with an accuracy of 89.95%

Fig. 3 compares GPR and LoR in estimating risk curves for IEEE 33-bus and 123-bus systems. Both models show similar risk estimations, confirming the consistency of our



(a) 33-bus



(b) 123-bus

Figure 3: Comparison between GPR and LoR used for predicting the risk index $R(x)$ on IEEE 33- and 123-bus systems, given different PV penetration levels (**No control**).

proposed models in classifying over-voltage issues. However, it is important to note that the LoR model cannot predict maximum voltage output like the GPR model. Therefore, the LoR model is solely used for calculating chance-constrained PV hosting capacity, while GPR can be applied for estimating the mean and bounds of HC as well as chance-constrained HC, as discussed in the next section.

GPR is non-parametric learning method, so the performance does not depend strongly on the input distribution. GPR has proven efficient on real-world datasets [7, 51], while LoR has been applied to actual water pipeline failure data [40]. In case the samples are not drawn from the assumptions of the probabilistic models, then we can apply transformation techniques like isoprobabilistic transforms, or Nataf transform before training the models [25].

4.3. Enhanced hosting capacity estimations with control techniques

In the previous section, the effectiveness of the proposed GPR and LoR methods have been verified, as shown in Tab. 2. In this section, we apply the GPR to estimate the mean and confident intervals for the HC, using the GP-WoCC-HC method proposed in (14)-(15), which does not consider the chance constraint. Subsequently, we present the results of chance-constrained HC using both GPR and LoR approaches, as proposed in (17) and (22), respectively.

We also estimated HC considering multiple control methods. The first two methods control the PV inverter's

Table 3

GP-WoCC-HC method for estimating means and 95% confident interval bounds of PV hosting capacity levels (in terms of % of the peak load).

	IEEE	Control	mean	lower	upper
33-bus		no	62.02%	44.20%	79.79%
		Q	71.12%	53.69%	92.38%
		PF	74.11%	55.95%	98.71%
123-bus		no	20.76%	10.76%	31.81%
		Q	36.22%	22.22%	54.85%
		PF	37.31%	18.89%	85.12%
		ESS	45.15%	31.30%	57.54%

output through Volt-Var (Q) control and power factor (PF) control. The droop characteristics and the control methodology are described in Module 4 of the Appendix. For the 123-bus system, we additionally evaluated HC under energy storage system (ESS) control. For this case study, the 123-bus was considered to be equipped with six ESS with power ratings of 150 (kW) each and located at bus [50, 70, 72, 80, 105, 110]. We assume that the control actions comply with the ESS state-of-charge limits.

Tab. 3 presents the estimated mean values of the PV HC for the IEEE 33-bus and 123-bus networks, along with the lower and upper bounds of HC at a 95% confidence level. Additionally, the effectiveness of enhanced control techniques, including PV inverter control and ESS control, are shown to increase the HC compared to results without control actions. Within the settings in this work, our findings indicate that PF control is more efficient than Q control in enhancing the HC in the IEEE 33-bus network, while the ESS technique outperforms PV inverter control in the IEEE 123-bus system. For instance, in the IEEE 33-bus network, the HC can be increased from a mean of 62.02% of the peak load of 3.715 (MW) to 71.12% on average with Q control, while PF control can improve the HC up to 74.11%. However, we observed that the PF control is only slightly better than the Q control in maximizing the HC mean value in the IEEE 123-bus network, but it also showed a great variance with the bounds ranging from a minimum of 18.89% to a maximum of 85.12%. The reason could be that the IEEE 123-bus is more compact with shorter branches than the IEEE 33-bus network.

Next, we present the estimation of chance-constrained HC, ensuring that the likelihood of over-voltage is at most risk levels of $\beta = 1\%$, 5% , and 10% . The results for all cases are shown in Table 4. As expected, the resulting CC-HC values are lower than the ones without the chance constraint due to the risk-averse nature of the optimization. For instance, at an extremely risk-averse level of $\beta = 1\%$, the GPR-based CC-HC in the IEEE 33-bus is only 40.56% of the peak load of 3.715 (MW). Meanwhile, the PF control technique can improve the GPR-based CC-HC up to 50.50%. Furthermore, we find that the logit-based model mostly provides smaller estimations compared to the GPR approach. Nevertheless, as the acceptable risk levels increase, the results from both models become closer, as seen in the case of $\beta = 10\%$ with the ESS control in the

Table 4

Comparison of GP-CC-HC and Logit-CC-HC methods for the estimation of chance-constrained PV hosting capacity levels.

IEEE	Control	Risk level β	GP-CC-HC	Logit-CC-HC
33-bus	no	1%	40.56%	34.19%
		5%	47.21%	43.84%
		10%	50.59%	48.21%
	Q	1%	50.50%	45.72%
		5%	56.43%	54.32%
		10%	59.59%	58.22%
	PF	1%	52.68%	46.71%
		5%	58.76%	56.05%
		10%	62.02%	60.28%
123-bus	no	1%	8.96%	4.49%
		5%	12.31%	10.33%
		10%	14.13%	12.97%
	Q	1%	20.22%	20.68%
		5%	24.06%	26.26%
		10%	26.35%	28.79%
	PF	1%	16.57%	4.75%
		5%	21.01%	16.80%
		10%	23.66%	22.25%
	ESS	1%	27.80%	28.66%
		5%	33.79%	34.57%
		10%	36.70%	37.24%

IEEE 123-bus, where the CC-HC is estimated to be 36.70% and 37.24% by the GP and logit learning approaches, respectively. One possible reason could be that as the risk level increases, the chance constraints become less restrictive. Note that our proposed methods take a total time of less than 3.24 seconds to generate 500 samples of the load flow, train the GPR and LoR models, and solve the proposed GP-CC-HC and logit-CC-HC optimizations for the estimations shown in Table 4.

Figures 4 and 5 display risk curves estimated by the LoR models for the IEEE 33-bus and by the GPR models for the IEEE 123-bus, respectively. These curves enable system operators to quickly determine the over-voltage risk at any PV penetration level in the networks, which is valuable for decision-making. Additionally, the figures demonstrate the effectiveness of Q, PF, and ESS control techniques in improving HC, as evidenced by the fact that at the same PV penetration level, the risks are reduced.

We further examine the estimated HC under various peak loads, as depicted in Fig. 6. Our findings indicate that as peak loads in networks rise, so do HC values. This trend holds even when considering enhancements like reactive power and energy storage system controls. Additionally, we observe instances where PF control proves more effective than Q control and even ESS control in the IEEE 123-bus network. This highlights the potential for further study and adjustment of PF control to maximize HC.

4.4. HC estimation with both solar PV and wind turbine units

We further utilized the proposed method to estimate the maximum renewable penetration when the network has both

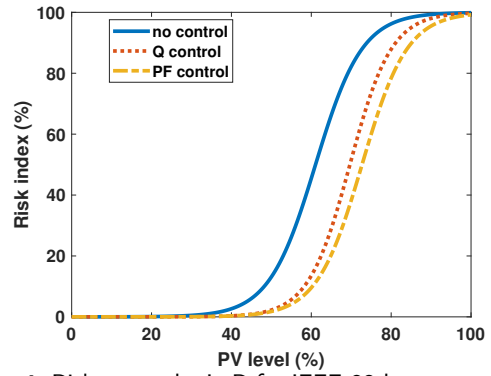


Figure 4: Risk curves by LoR for IEEE 33-bus system, considering the reactive power (Q) and power factor (PF) controls.

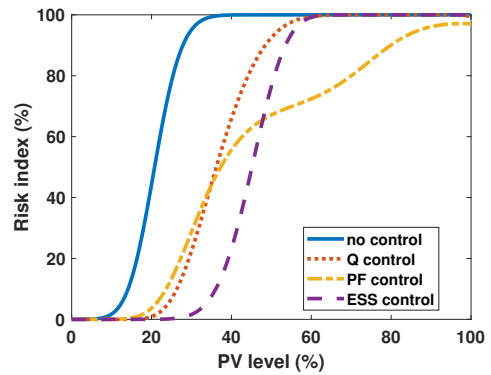


Figure 5: Risk curves by GPR for IEEE 123-bus system, considering the reactive power (Q), power factor (PF), and energy storage system (ESS) controls.

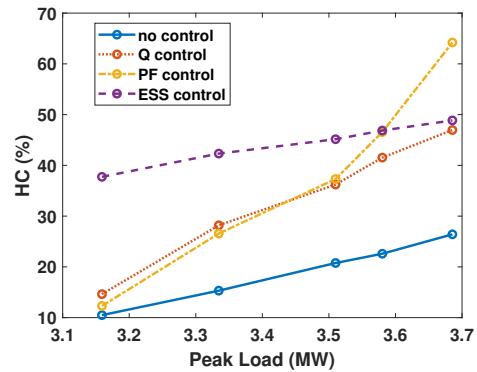


Figure 6: Estimating the mean values of the HC for the IEEE 123-bus system, considering different peak loads.

solar PV and wind turbine (WT) units. For a given level of solar PV and WT penetration, we randomly allocate these units to different buses using the method given in Appendix. We also considered the correlation between PV and WT units using copula function as shown in the Appendix. The results of variation in risk index with PV and wind turbine penetration is shown in Fig. 7. The data for this case study was taken from reference [39]. Further, we estimate the maximum WT penetration for a given penetration of solar PV and a given risk index levels. The results are shown in Table 5. It can be observed that the amount of WT hosted by the network reduces if the penetration of PV increases.

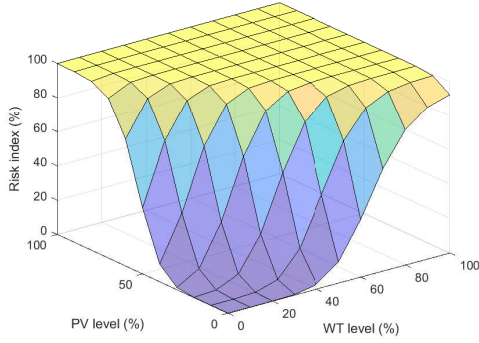


Figure 7: Variation in risk index with penetration levels of solar PV and wind turbine units

Table 5
GP-CC-HC estimation for PV and WT (%) at risk index 5%.

Risk level β	PV	WT
5%	10%	29.33%
	20%	19.33%
	30%	9.33%

4.5. Notes on comparison with the existing method

In this section, we aim to briefly compare our proposed methods with [24], where the authors employed a polynomial chaos expansion (PCE)-based chance-constrained probabilistic optimal power flow (PCE-CC-POPF) method. While both methods are effective for HC estimation in distribution networks, they exhibit differences in approach.

Firstly, the complexity of our proposed methods is relatively lower. We utilize a modest sample size, like $n_s = 500$, for probabilistic load flow, then employ GPR and LoR models to predict over-voltage risk. Our chance-constrained optimization is solved with a straightforward objective function and univariate constraint. In contrast, the approach in [24] is more complex, involving CC-POPF with multiple constraints and requiring simultaneous determination of coefficients for several PCE models.

Secondly, our proposed methods demonstrate superior computational efficiency. The GPR models are trained offline and can be applied to any nonlinear relationship with any distributions of correlated uncertain loads and renewable generations, and once the models are built, the online computation for predicting the HC values with different associated risks is fast and simple. In contrast, the general PCE-based POPF approach often encounters the “*curse of dimensionality*” and relies on the assumption of independent inputs [29]. Thus, in practice, the degree of general multivariate PCEs is usually restricted to an order of 2 only. For highly nonlinear and correlated input scenarios, obtaining coefficients for general PCE models can be computationally intensive and time-consuming. Our methods, tested on IEEE 33-bus and 123-bus systems, complete the process of HC estimation in under 3.24 seconds (including training data generation), while the PCE-CC-POPF method in [24] takes around 4.04 seconds for similar tasks, see Tab. III in [24] for more time comparisons with other approaches.

Table 6

The pros and cons of the GP-based and the logit-based chance-constrained HC estimation methods.

Method	Pros	Cons
GP	Captures non-linearity Non-parametric nature Uncertainty quantification More robust to outliers Smoothness assumptions	Computational complexity Scalability issues Hyperparameter tuning
Logit	Simplicity and interpretability Computational efficiency	Linear decision boundary Sensitivity to outliers Limited to binary outcomes

4.6. Notes on pros and cons of the two proposed CC-HC estimation methods

In this subsection, we provide a comparison of the pros and cons of the GP-based and logit-based HC estimation methods, as shown in Table 6.

The GP model is a non-parametric method, thus it does not assume a fixed form for the underlying function, allowing it to model complex, non-linear relationships effectively. Additionally, the GP-based method offers uncertainty quantification in predictions and is more robust to outliers, which is particularly useful in chance-constrained HC assessment where uncertainty is a critical factor. Furthermore, the GP assumes smoothness in the underlying function, making it well-suited for modelling continuous maximum voltage outputs, without the need to handle unbalanced data (e.g. zero-inflated binary outcomes) as in the logistic regression. However, the GP approach comes with higher computational costs and scalability issues, especially for large datasets, as it involves inverting large covariance matrices. These issues can be solved by using sparse GP. In addition, the GP approach requires careful choosing kernel functions and tuning of their hyperparameters, which can be complex and time-consuming.

On the other hand, the logit-based method is simpler, more interpretable, and computationally efficient with large datasets. However, it may not capture complex relationships as effectively as GP, and it can be sensitive to outliers, owing to the assumption of a linear relationship between the predictor (i.e. the PV level) and the log-odds of the over-voltage event. Moreover, we need to apply zero-inflated models if the response variable contains an excess of zeros, such as in cases where violation events rarely occur.

5. Conclusion

In this study, we proposed the chance-constrained PV HC estimation of distribution networks using Gaussian process regression and logistic regression. Our results showed that the GPR and LoR models can achieve high accuracy ranging from 90%-93% in predicting nodal over-voltage events in the IEEE 33 and 123-bus systems. Thus, they can be effectively applied to estimate the chance-constrained HC with different risk levels, especially the GPR can offer the mean values and confidence interval bounds for the HC estimation. Moreover, our proposed methods have simple forms and low computational costs with the total time spent of only a few seconds. In this work, we also confirmed

that the use of Q, PF, and ESS controls can improve the HC of distribution networks. Our research has significant implications for the energy sector, aiding system operators in optimizing the integration of PV systems into distribution networks.

Appendix

This appendix outlines the methodology for generating maximum voltage data for a given PV penetration level. Fig. 8 depicts the flowchart of the procedure.

Module 1: Representative load-generation profiles

In this module, we sample uncertain load and PV output (normalized). These normalized values can be multiplied with base values to obtain a random scenario for analysis. Let F_1 and F_2 be CDFs of the normalized load P_{dn} and normalized PV generation P_{gn} . Then by Sklar's theorem in the copula theory [45], there exists a unique copula function C capturing the dependence structure/correlation between the variable P_{dn} and P_{gn} such that the joint CDF defined by:

$$\begin{aligned} H(p_1, p_2) &:= \mathbb{P}(P_{dn} \leq p_1, P_{gn} \leq p_2) \\ &= C(F_1(p_1), F_2(p_2)). \end{aligned} \quad (23)$$

It is well-known that if P_{dn} and P_{gn} are independent, then their copula is $C(u_1, u_2) = u_1 u_2$, and we have the joint CDF: $H(p_1, p_2) = F_1(p_1) F_2(p_2)$ [45]. For the sake of simplicity, we shall use a Gaussian copula $C_\rho(u_1, u_2)$, where ρ is the copula parameter (Pearson's correlation coefficient). Also, we take the marginal CDFs F_1 and F_2 as normal $\mathcal{N}(0.5, 0.025^2)$ and Beta(15, 6) distributions, respectively. Now, we can generate the representative load and generation profiles as follows:

- (i) Generate M random samples using estimated copula:

$$(u_1^j, u_2^j) \sim C_\rho, j = 1, \dots, M.$$

- (ii) Get normalized load and PV generation profiles by:

$$P_{dn}^j = F_1^{-1}(u_1^j), \quad P_{gn}^j = F_2^{-1}(u_2^j), j = 1, \dots, M.$$

- (iii) Multiply normalized values with base values.

In this work, we have not included spatial correlation explicitly. Since the size of a distribution network is rather small, it seems reasonable to assume uniform solar conditions.

Module 2: Generating location and size scenarios

In this module, we create L location-size scenarios of the PV unit installations. Let PV^{loc} be the set of candidate buses at which PV units can be installed with N^{pv} being the set size. For each scenario i in the set L , firstly, a vector u is initialized. This vector represents the size of the PV unit installed at each bus. Next, the total number of buses having PV units (denoted as K) is obtained randomly from a discrete uniform distribution. This is followed by randomly selecting K unique integers from the set loc to formulate the set PV^{loc} of random location scenarios. Finally, for each

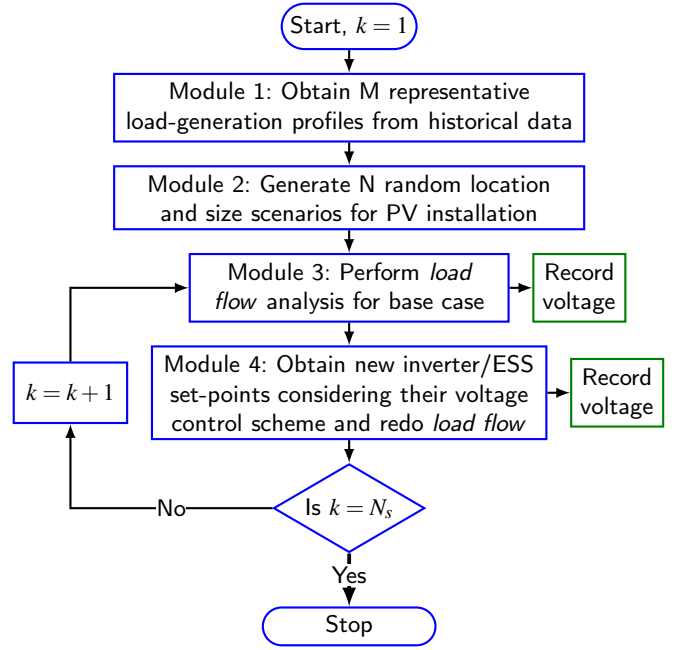


Figure 8: Flowchart of the data generation process.

bus in the set PV^{loc} , the PV is sized by generating a random number between 0 and ζ using the uniform distribution. We have limited the PV installed at each bus to 1.5 times the peak load for realistic analysis.

Module 3: Base case load flow

After obtaining location-size scenarios from Module 2, load flow analysis is performed. For each scenario, M load flows are performed corresponding to M representative load-generation profiles. The PV output at each bus is derived by multiplying the PV size at that bus by the normalized generation values from Module 1. This PV output is then subtracted from the load to determine the net load. Further, the reactive power from the PV inverter is considered to be 0 in this module.

Module 4: Load flow considering PV inverter/ESS control

In this module, we consider the case where the PV inverters are equipped with a localized voltage control algorithm. The voltages obtained from base-case load flow (i.e. Module 3) are the voltages sampled by the PV inverters. Based on this measured voltage, a new set-point is obtained based on the control algorithm. In this work, we have considered Volt-Var (Q) control and power factor (PF) control [21]. The Volt-Var technique to control voltages is as follows:

$$Q_{pv,i} = \begin{cases} Q_{max,i}, & \text{if } V_i \leq v_1, \\ \frac{V_i - v_2}{v_1 - v_2} Q_{max,i}, & \text{if } v_1 < V_i \leq v_2, \\ 0, & \text{if } v_2 < V_i < v_3, \\ -\frac{V_i - v_3}{v_4 - v_3} Q_{max,i}, & \text{if } v_3 \leq V_i < v_4, \\ -Q_{max,i}, & \text{if } V_i \geq v_4, \end{cases} \quad (24)$$

$$Q_{max,i} = \sqrt{S_{max,i}^2 - P_{pv,i}^2}$$

where $P_{pv,i}$ is the active power output of the PV unit and $S_{max,i}$ is the inverter rating. In this work, we have assumed an inverter rating equal to the PV unit size. It can be observed that there is no curtailment of active power in this method. The values of (v_1, \dots, v_4) are (0.95, 0.97, 1.03, 1.05) per unit.

Next, we consider the case of the adaptive power factor method. In this method, the PV inverter changes its power factor according to the voltage value as follows:

$$PF_{pv,i} = \begin{cases} 1, & \text{if } V_i \leq v_3, \\ c_1 + \frac{1-c_1}{v_3-v_4} (V_i - v_4), & \text{if } v_3 < V_i < v_4, \\ c_1, & \text{if } V_i \geq v_4, \end{cases} \quad (25)$$

where c_1 is chosen as 0.95 in this work.

Lastly, we define the voltage control using ESS as follows:

$$P_{ess,i} = \begin{cases} P_{max,i}, & \text{if } V_i \leq v_1, \\ \frac{V_i - v_2}{v_1 - v_2} P_{max,i}, & \text{if } v_1 < V_i \leq v_2, \\ 0, & \text{if } v_2 < V_i < v_3, \\ -\frac{V_i - v_3}{v_4 - v_3} P_{max,i}, & \text{if } v_3 \leq V_i < v_4, \\ -P_{max,i}, & \text{if } V_i \geq v_4, \end{cases} \quad (26)$$

where $P_{max,i}$ is the rated power output of i^{th} ESS. We considered 6 ESS with a rating of 150 kW each and located at bus [50, 70, 72, 80, 105, 110] in the 123-bus network. A negative sign signifies ESS charging.

Finally, similar to Module 3, load flow analysis is performed after adjusting the PV unit's output into active/reactive power demand at each bus. The control procedure iterates until convergence, defined as the maximum voltage magnitude difference between iterations being less than ϵ_v (0.005). The detailed procedure of voltage control in Module 4 is provided in the algorithm (Algorithm 1).

Algorithm 1 Module 4: Obtain new setpoints for PV inverter/ESS and re-perform load flow

```

1: Input:  $V, \epsilon_v$ 
2: Initialize:  $\Delta V = \mathbf{0}, err = 1,$ 
3: Output:  $P_{pv}, Q_{pv}$ 
4: while  $err > \epsilon_v$  do
5:   for each bus do
6:     Obtain new PV inverter/ ESS set-points using (24)
       / (25) / (26).
7:   end for
8:   Using new inverter/ ESS set-points, obtain bus volt-
     ages ( $V_n$ ) using load flow analysis.
9:    $err = \max(|V - V_n|)$ 
10:   $V = V_n$ 
11: end while

```

References

[1] A. Ali, K. Mahmoud, and M. Lehtonen. Maximizing hosting capacity of uncertain photovoltaics by coordinated management of oltc, var sources and stochastic evs. *International Journal of Electrical Power & Energy Systems*, 127:106627, 2021.

- [2] M. Ali, E. Gryazina, A. Dymarsky, and P. Vorobev. Calculating voltage feasibility boundaries for power system security assessment. *International Journal of Electrical Power & Energy Systems*, 146:108739, 2023.
- [3] A. Arshad and M. Lehtonen. A stochastic assessment of pv hosting capacity enhancement in distribution network utilizing voltage support techniques. *IEEE Access*, 7:46461–46471, 2019.
- [4] M. S. Ayaz, M. Malekpour, R. Azizipanah-Abarghooee, M. Karimi, and V. Terzija. Probabilistic photovoltaic generation and load demand uncertainties modelling for active distribution networks hosting capacity calculations. *International Journal of Electrical Power & Energy Systems*, 159:110016, 2024.
- [5] M. E. Baran and F. F. Wu. Network reconfiguration in distribution systems for loss reduction and load balancing. *IEEE Transactions on Power Delivery*, 4(2):1401–1407, 1989.
- [6] L. Bobo, A. Venzke, and S. Chatzivasileiadias. Second-order cone relaxations of the optimal power flow for active distribution grids: Comparison of methods. *International Journal of Electrical Power & Energy Systems*, 127:106625, 2021.
- [7] H. Cai, X. Jia, J. Feng, W. Li, Y.-M. Hsu, and J. Lee. Gaussian process regression for numerical wind speed prediction enhancement. *Renewable energy*, 146:2112–2123, 2020.
- [8] G. W. Chang, N. C. Chinh, and C. Sinatra. Equilibrium optimizer-based approach of pv generation planning in a distribution system for maximizing hosting capacity. *IEEE Access*, 10:118108–118122, 2022.
- [9] M. J. Chihota, B. Bekker, and T. Gaunt. A stochastic analytic-probabilistic approach to distributed generation hosting capacity evaluation of active feeders. *International Journal of Electrical Power & Energy Systems*, 136:107598, 2022.
- [10] Y. Cho, E. Lee, K. Baek, and J. Kim. Stochastic optimization-based hosting capacity estimation with volatile net load deviation in distribution grids. *Applied Energy*, 341:121075, 2023.
- [11] L. Chuan and A. Ukil. Modeling and validation of electrical load profiling in residential buildings in singapore. *IEEE Transactions on Power Systems*, 30(5):2800–2809, 2015.
- [12] F. Ding and B. Mather. On distributed pv hosting capacity estimation, sensitivity study, and improvement. *IEEE Transactions on Sustainable Energy*, 8(3):1010–1020, 2016.
- [13] A. Dubey and S. Santoso. On estimation and sensitivity analysis of distribution circuit's photovoltaic hosting capacity. *IEEE Transactions on Power Systems*, 32(4):2779–2789, 2016.
- [14] P. Eleftheriadis, M. Gangi, S. Leva, A. V. Rey, E. Groppo, and L. Grande. Comparative study of machine learning techniques for the state of health estimation of li-ion batteries. *Electric Power Systems Research*, 235:110889, 2024.
- [15] D. Eltigani and S. Masri. Challenges of integrating renewable energy sources to smart grids: A review. *Renewable and Sustainable Energy Reviews*, 52:770–780, 2015.
- [16] E. Erdođan and G. Iyengar. Ambiguous chance constrained problems and robust optimization. *Mathematical Programming*, 107:37–61, 2006.
- [17] F. Y. Ettoumi, A. Mefi, A. Adane, and M. Bouroubi. Statistical analysis of solar measurements in algeria using beta distributions. *Renewable Energy*, 26(1):47–67, 2002.
- [18] A. Geletu, M. Klöppel, H. Zhang, and P. Li. Advances and applications of chance-constrained approaches to systems optimisation under uncertainty. *International Journal of Systems Science*, 44(7):1209–1232, 2013.
- [19] J. M. Home-Ortiz, L. H. Macedo, R. Vargas, R. Romero, J. R. S. Mantovani, and J. P. Catalao. Increasing res hosting capacity in distribution networks through closed-loop reconfiguration and volt/var control. *IEEE Trans. on Industry Applications*, 58(4), 2022.
- [20] T. Huld, R. Müller, and A. Gambardella. A new solar radiation database for estimating pv performance in europe and africa. *Solar energy*, 86(6):1803–1815, 2012.
- [21] I. A. Ibrahim and M. Hossain. A benchmark model for low voltage distribution networks with pv systems and smart inverter

- control techniques. *Renewable and Sustainable Energy Reviews*, page 112571, 2022.
- [22] W. Jiao, Q. Wu, J. Chen, J. Tan, G. Song, S. Huang, and C. Wang. Analytical target cascading based real-time distributed voltage control for mv and lv active distribution networks. *International Journal of Electrical Power & Energy Systems*, 159:110024, 2024.
- [23] A. Kharrazi, V. Sreeram, and Y. Mishra. Assessment techniques of the impact of grid-tied rooftop photovoltaic generation on the power quality of low voltage distribution network—a review. *Renewable and Sustainable Energy Reviews*, 120:109643, 2020.
- [24] A. Koirala, T. Van Acker, M. U. Hashmi, R. D’hulst, and D. Van Hertem. Chance-constrained optimization based pv hosting capacity calculation using general polynomial chaos. *IEEE Trans. on Power Systems*, 2023.
- [25] R. Lebrun and A. Duffoy. A generalization of the nataf transformation to distributions with elliptical copula. *Probabilistic Engineering Mechanics*, 24(2):172–178, 2009.
- [26] J. Li, S. Ge, H. Liu, T. Hou, P. Wang, and P. Xing. An improved igdt approach for distributed generation hosting capacity evaluation in multi-feeders distribution system with soft open points. *International Journal of Electrical Power & Energy Systems*, 154:109404, 2023.
- [27] H. Liu, Y.-S. Ong, X. Shen, and J. Cai. When gaussian process meets big data: A review of scalable gps. *IEEE transactions on neural networks and learning systems*, 31(11):4405–4423, 2020.
- [28] R. Liuyacc-Blas, M. L. Kolhe, and P. Kepplinger. Enhanced violation-mitigation-based method using voltage/current sensitivities for pv hosting capacity quantification in low-voltage grids. *Electric Power Systems Research*, 232:110430, 2024.
- [29] S. Ly, P. Pareek, and H. D. Nguyen. Scalable probabilistic optimal power flow for high renewables using lite polynomial chaos expansion. *IEEE Systems Journal*, 17(2):2282–2293, 2023.
- [30] M. Mitrovic, A. Lukashovich, P. Vorobev, V. Terzija, S. Budenny, Y. Maximov, and D. Deka. Data-driven stochastic ac-opf using gaussian process regression. *International Journal of Electrical Power & Energy Systems*, 152:109249, 2023.
- [31] V. C. Moro, F. C. Trindade, F. B. Costa, and B. D. Bonatto. Distributed generation hosting capacity analysis: An approach using interval-affine arithmetic and power flow sensitivities. *Electric Power Systems Research*, 226:109946, 2024.
- [32] E. Mulenga, M. H. Bollen, and N. Etherden. Solar pv stochastic hosting capacity in distribution networks considering aleatory and epistemic uncertainties. *International Journal of Electrical Power & Energy Systems*, 130, 2021.
- [33] S. Munikoti, M. Abujubbeh, K. Jhala, and B. Natarajan. A novel framework for hosting capacity analysis with spatio-temporal probabilistic voltage sensitivity analysis. *International Journal of Electrical Power & Energy Systems*, 134:107426, 2022.
- [34] H. D. Nguyen, K. Dvijotham, and K. Turitsyn. Constructing convex inner approximations of steady-state security regions. *IEEE Trans. on Power Systems*, 34(1):257–267, 2018.
- [35] H. D. Nguyen and K. Turitsyn. Voltage multistability and pulse emergency control for distribution system with power flow reversal. *IEEE Transactions on Smart Grid*, 6(6):2985–2996, 2015.
- [36] P. Pareek and H. D. Nguyen. Gaussian process learning-based probabilistic optimal power flow. *IEEE Transactions on Power Systems*, 36(1):541–544, 2020.
- [37] P. Pareek and H. D. Nguyen. A framework for analytical power flow solution using gaussian process learning. *IEEE Transactions on Sustainable Energy*, 13(1):452–463, 2022.
- [38] P. Pareek, W. Yu, and H. D. Nguyen. Optimal steady-state voltage control using gaussian process learning. *IEEE Transactions on Industrial Informatics*, 17(10):7017–7027, 2020.
- [39] Z. Qin, W. Li, and X. Xiong. Incorporating multiple correlations among wind speeds, photovoltaic powers and bus loads in composite system reliability evaluation. *Applied energy*, 110:285–294, 2013.
- [40] A. Robles-Velasco, P. Cortés, J. Muñuzuri, and L. Onieva. Prediction of pipe failures in water supply networks using logistic regression and support vector classification. *Reliability Engineering & System Safety*, 196:106754, 2020.
- [41] E. Schulz, M. Speekenbrink, and A. Krause. A tutorial on gaussian process regression: Modelling, exploring, and exploiting functions. *Journal of mathematical psychology*, 85:1–16, 2018.
- [42] S. R. Sinsel, R. L. Riemke, and V. H. Hoffmann. Challenges and solution technologies for the integration of variable renewable energy sources—a review. *renewable energy*, 145:2271–2285, 2020.
- [43] S. Solat, F. Aminifar, and H. Shayanfar. Distributed generation hosting capacity in electric distribution network in the presence of correlated uncertainties. *IET Generation, Transmission & Distribution*, 15(5):836–848, 2021.
- [44] S. Talkington, S. Grijalva, M. J. Reno, J. A. Azzolini, and D. Pinney. A measurement-based approach to voltage-constrained hosting capacity analysis with controllable reactive power behind-the-meter. *Electric Power Systems Research*, 221:109395, 2023.
- [45] P. K. Trivedi, D. M. Zimmer, et al. Copula modeling: an introduction for practitioners. *Foundations and Trends® in Econometrics*, 1(1):1–111, 2007.
- [46] S. Wang, Y. Dong, L. Wu, and B. Yan. Interval overvoltage risk based pv hosting capacity evaluation considering pv and load uncertainties. *IEEE transactions on smart grid*, 11(3):2709–2721, 2019.
- [47] Y. Weng, S. Yu, K. Dvijotham, and H. D. Nguyen. Fixed-point theorem-based voltage stability margin estimation techniques for distribution systems with renewables. *IEEE Transactions on Industrial Informatics*, 18(6):3766–3776, 2021.
- [48] C. K. Williams and C. E. Rasmussen. *Gaussian processes for machine learning*, volume 2. MIT press Cambridge, MA, 2006.
- [49] H. Wu, Y. Yuan, X. Zhang, A. Miao, and J. Zhu. Robust comprehensive pv hosting capacity assessment model for active distribution networks with spatiotemporal correlation. *Applied Energy*, 323:119558, 2022.
- [50] H. Yao, W. Qin, X. Jing, Z. Zhu, K. Wang, X. Han, and P. Wang. Possibilistic evaluation of photovoltaic hosting capacity on distribution networks under uncertain environment. *Applied Energy*, 324, 2022.
- [51] A. Zeng, H. Ho, and Y. Yu. Prediction of building electricity usage using gaussian process regression. *Journal of Building Engineering*, 28:101054, 2020.
- [52] H. Zhang and P. Li. Chance constrained programming for optimal power flow under uncertainty. *IEEE Transactions on Power Systems*, 26(4):2417–2424, 2011.
- [53] L. Zhang, H. Ye, F. Ding, Z. Li, and M. Shahidehpour. Increasing pv hosting capacity with an adjustable hybrid power flow model. *IEEE Transactions on Sustainable Energy*, 14(1):409–422, 2022.
- [54] S. Zhang, S. Ge, H. Liu, G. Hou, and C. Wang. An analytical method for delineating feasible region for pv integration capacities in net-zero distribution systems considering battery energy storage system flexibility. *Journal of Modern Power Systems and Clean Energy*, 2024.
- [55] S. Zhang, S. Ge, H. Liu, J. Li, and C. Wang. Model and observation of the feasible region for pv integration capacity considering wasserstein-distance-based distributionally robust chance constraints. *Applied Energy*, 347:121312, 2023.